

Pb(II) and As(V) ion Partitioning at Polymer Film – Metal Oxide Interfaces: A Long-Period X-ray Standing Wave Study

Tae Hyun Yoon¹, Thomas P. Trainor², Peter J. Eng³ and Gordon E. Brown, Jr.^{1,4}

¹ Department of Geological & Environmental Sciences, Stanford University, Stanford, CA 94305-2115, USA;

² Department of Chemistry and Biochemistry, University of Alaska Fairbanks, Fairbanks, AK 99775, USA.;

³ GSECARS, University of Chicago, Chicago, IL 60637, USA;

⁴Stanford Synchrotron Radiation Laboratory, SLAC, Menlo Park, CA 94025, USA

Introduction

Solid-water interfaces are of great significance in many areas of science and engineering, including aqueous geochemistry, contaminant transport in groundwater, waste water treatment, heterogeneous catalysis, atmospheric aerosol chemistry, corrosion science, and colloid science^{1,2}. Moreover, in many natural settings, natural organic matter (NOM) is ubiquitous, and can form coatings on mineral surfaces that may cause significant changes in interfacial properties³⁻¹². NOM coatings on mineral surfaces can act as (1) a competing sorbent for pollutant ion species, (2) a physical barrier inhibiting the transport of ions to mineral surface binding sites, (3) a passivating layer blocking high affinity surface sites, and/or (4) a charged medium that modifies the electrical double layer properties at the mineral-water interface. As a consequence, NOM coatings on mineral surfaces may cause dramatic changes in many of the physicochemical properties of mineral particles, including their sorption capacity and reactivity to various pollutant ions and the kinetics of sorption/desorption reactions. However, due mainly to experimental difficulties in probing trace element distributions at organic film – mineral interfaces under *in situ* conditions, only a few such studies have been conducted⁸⁻¹², and thus our knowledge of these distributions is limited.

The long-period x-ray standing wave method, combined with x-ray reflectivity measurements, is well suited for probing trace element distributions within thin organic film layers (> 10 nm) on polished metal oxide surfaces under *in situ* conditions¹³⁻¹⁹. Previous long-period XSW studies^{13-15,17-19} have shown the utility of this technique for determining metal ion distributions within a variety of model organic films and biofilms on reflecting mirror substrates under *in situ* conditions. In order to derive a more quantitative understanding of the partitioning behavior of common pollutants ions [e.g., Pb(II) and As(V)] at mineral/NOM/water interfaces, a reductionist approach is needed due to the complexity of NOM. In this study, using the long-period x-ray standing wave (XSW) technique, combined with x-ray reflectivity measurements, we quantitatively determined the partitioning ratios of Pb(II) and/or As(V)O₄³⁻ ions at PAA/ α -Al₂O₃(0001), PAA/ α -Al₂O₃(1-102), and PAA/ α -Fe₂O₃(0001) interfaces. The main objective of this study is to determine the effect of a continuous PAA coating on different metal oxide surfaces on the partitioning behavior of these aqueous ions.

Methods and Materials

Sample Preparation. The mineral surfaces used in these experiments were commercially available, highly polished, 2-inch diameter synthetic (0001) and (1-102) α -Al₂O₃ single crystals (Saint-Gobain Crystals & Detectors Co), and natural (0001) α -Fe₂O₃ single crystals (Commercial Crystal Laboratory, Inc.). PAA thin films containing Pb(II) or As(V)O₄³⁻ ions were prepared on these single crystals by using a spin-coating method. For XSW sample preparation, aliquots of PAA stock solution and Pb(II)(NO₃)₂ (Aldrich Chemical Co.

Ltd.) or Na₂HAs(V)O₄ (Alfa Aesar) solution were mixed to make final solutions with specific [PAA], [Pb(II)] and/or [As(V)O₄³⁻]. The pH of each solution was adjusted to 4.5 using 1 M NaOH and 1 M HCl. 600 μ l of these solutions were placed on the single crystal substrates and were equilibrated for 2 hours before the spin drying process. Spin coating was performed using a Headway Research Inc., EC101DT spinner operated at 2000 rpm for 60 seconds. The resulting PAA-coated crystals were kept under a dry N₂ atmosphere prior to XSW-FY and x-ray reflectivity measurements at the Advanced Photon Source (APS).

Data Collection and Processing. Long-period XSW-FY and x-ray reflectivity measurements were performed at the GSECARS sector at the APS on undulator beamline 13-ID-C using a liquid N₂ cooled Si(111) monochromator with Rh-coated double focusing mirrors. The x-ray beam was collimated to 1.7 mm vertical and 10 μ m horizontal. The samples were placed in a Teflon sample cell covered with polypropylene film and the space over the sample was purged by dry He gas during experiments. The x-ray incidence angle was scanned between 0.0 and 1.0 degree for the x-ray reflectivity measurements while the incident (I₀) and reflected (I₁) x-rays were monitored by using N₂-filled gas ionization chambers. Pb L _{α} and As K _{α} XSW-FY spectra were collected using 14 keV and 13 keV incident x-ray energies, respectively, and the spectra were processed using the following protocol. Fluorescence spectra were acquired using a 13-element Ge array detector (Canberra) coupled to digital X-ray processor (DXP) electronics (X-ray Instrumentation Associates) as the incidence angle was changed from 0.02 to 0.32 degrees in 0.002° or 0.005° steps. The fluorescence yield spectrum from each detector element was averaged with the other spectra and deadtime corrected. The total area of Pb L _{α} and As K _{α} fluorescence peaks located around 10.5 keV were fit using a Gaussian peak lineshape on a linear background¹⁸.

Analysis of XSW and Reflectivity Data. X-ray reflectivity curves were used to estimate the thicknesses of the PAA film and the roughnesses of the PAA/air and mineral/PAA interfaces, which were fixed or highly constrained input parameters in the XSW-FY curve fitting in the following step. The x-ray reflectivity data were fit using a 3-layer model: mineral substrate/PAA/air. The density of the PAA layer was constrained in the range of 1.35 to 1.65 g/cm³ during the reflectivity fitting procedure. A Debye-Waller model was used to account for interfacial roughness. The FY data were fit starting with parameters obtained from previous x-ray reflectivity curve fitting (i.e. the PAA film thickness, surface and interface roughness, and beam convolution factor). These parameters were fixed or highly constrained within narrow ranges during the XSW-FY curve fitting procedure. Details of the XSW-FY experimental setup and modeling have been previously described by Trainor et al.¹⁸ and Yoon et al.²⁰

Results and Discussion

Comparison of Pb(II) and As(V) Distributions at the PAA/ α -Al₂O₃(1-102) Interface. Figure 1 shows the x-ray reflectivity and XSW-FY profiles collected for Pb(II) and As(V)O₄³⁻ (both at 5 x 10⁻⁷ M) at the PAA/ α -Al₂O₃(1-102) interface. Considering the pH of the aqueous solution (4.5), the point of zero charge (pzc) of the α -Al₂O₃(1-102) surface (5.85)²¹, and the pK_a of PAA carboxyl groups (4.68)^{22,23}, the α -Al₂O₃ surface is expected to be positively charged while carboxyl functional groups in the PAA layer should be slightly negatively charged. Under these conditions, Pb(II) and As(V)O₄³⁻ are expected to show distinctly different partitioning

behavior at this interface. For example, Pb(II) should prefer to be associated with negatively charged carboxyl functional groups in the PAA film, based on electrostatic considerations alone, while As(V)O₄³⁻ will be repelled by the negatively charged functional groups in the PAA film and should prefer to adsorb on the positively charged α -Al₂O₃(1-102) surface at pH 4.5. The XSW-FY results shown in Fig. 1 are in good agreement with these predictions.

Curve fitting results of XSW-FY profiles show that most of the Pb(II) cations partition into the PAA film while the As(V)O₄³⁻ oxoanions are dominantly bound to the α -Al₂O₃(1-102) surface, suggesting the possible role of electrostatic interactions in the partitioning of Pb(II) and As(V)O₄³⁻ ions in this system. In addition to this electrostatic interaction, previous studies have indicated that a ML₂ type species is the dominant Pb(II) complex in PAA over a wide range of pH's including our experimental conditions ([Pb(II)] = 1 x 10⁻⁷ M, pH = 4.5)^{22,24}. These high affinity binding sites in PAA are also responsible for the partitioning of Pb(II) in this composite system.

As for the partitioning of As(V)O₄³⁻ oxoanions at the PAA/ α -Al₂O₃(1-102) interface, we observed that even though the carboxylate ligands in PAA have a much higher concentration than aqueous arsenate oxoanions ([COO⁻]_{PAA} = 0.21 M; [As(V)O₄³⁻] = 5 x 10⁻⁷ M) in our experiments, As(V)O₄³⁻ oxoanions occur dominantly at the PAA/ α -Al₂O₃(1-102) interface, probably due to the formation of stronger inner-sphere mode As(V)O₄³⁻ surface complexes at the aluminum oxide surface, as previously suggested by Arai *et al.*²⁵. This observation leads to two conclusions: (1) the surface binding sites of α -Al₂O₃(1-102) are not blocked by the PAA film and (2) AsO₄³⁻ oxoanions out-compete PAA carboxyl groups for reactive sites on the α -Al₂O₃(1-102) surface.

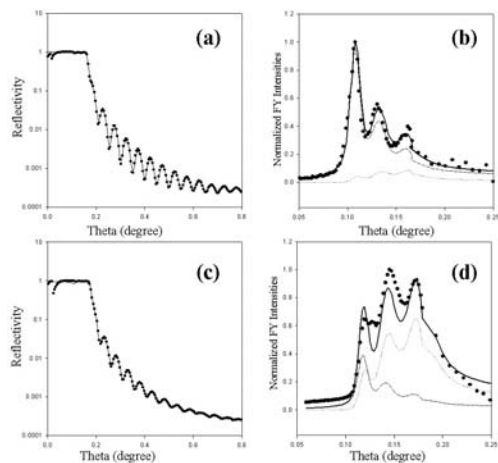


Figure 1. X-ray reflectivity [(a) and (c)] and XSW-FY profiles [(b) and (d)] of the PAA/ α -Al₂O₃(1-102) samples containing 5 x 10⁻⁷ M Pb(II) taken at an x-ray excitation energy of 14 keV [(a) and (b)] and 5 x 10⁻⁷ M As(V) taken at an x-ray excitation energy of 13 keV [(c) and (d)]. Filled circles: experimental data, solid line: best fit results, dotted line: XSW-FY components from adsorbed species, dashed line: XSW-FY components from PAA film bound species.

Effect of [Pb(II)] on Lead Partitioning at the PAA/ α -Al₂O₃(1-102) Interface. Experiments were also conducted on Pb(II) partitioning at the PAA/ α -Al₂O₃(1-102) interface as a function of Pb(II) concentration. As shown in Fig. 2, the XSW-FY profiles indicate that Pb(II) partitions dominantly into the PAA coating at [Pb(II)] = 5 x 10⁻⁸ M, and increasingly onto the α -Al₂O₃(1-102) surface with increasing Pb concentration, although the PAA coating remains the dominant sink for Pb even at [Pb(II)] = 2 x 10⁻⁵ M. The effect of [Pb(II)] on Pb(II) partitioning at a biofilm/ α -Al₂O₃(1-102) interface has been reported previously by Templeton *et al.*¹⁴. This earlier XSW-FY

study, which was conducted at pH 6, showed that the partitioning preference of Pb(II) ions switched from the α -Al₂O₃(1-102) surface to the *B. cepacia* biofilm coating as lead concentration increased from 10⁻⁶ M to 10⁻⁵ M, implying the presence of a limited number of binding sites at the α -Al₂O₃(1-102) surface with stronger affinity for the Pb(II) cation and large number of weaker binding site in *B. cepacia* biofilm. Our observations of Pb(II) partitioning at the PAA/ α -Al₂O₃(1-102) interface (see Fig. 2) indicate an opposite trend. Considering only electrostatic interactions of Pb(II) cations with the alumina surface under the condition examined, this is not surprising as the surface charge of α -Al₂O₃(1-102) should be positive at pH 4.5, resulting in repulsive interactions with Pb(II); in contrast, the carboxyl functional groups in PAA should be negatively charged, thus attracting Pb(II) cations. At pH 6 in the Pb(II)/biofilm- α -Al₂O₃ XSW-FY study, the alumina surface should be slightly negatively charged, resulting in attractive electrostatic interactions between Pb(II) and the surface sites.

However, Pb(II) cations should also form covalent bonds with the α -Al₂O₃(1-102) surface and PAA carboxyl groups (i.e., formation of inner-sphere complexes). Previous studies have shown that the adsorption mode of Pb(II) to high affinity binding sites at the α -Al₂O₃(1-102) surface (at pH = 6) is dominantly inner-sphere¹⁴. Although this inner-sphere type of binding is electrostatically unfavorable at pH 4.5, there should be some inner-sphere adsorption of Pb(II) at the α -Al₂O₃(1-102) surface, which is demonstrated by the distribution of Pb(II) in Figs. 2(b) and (c).

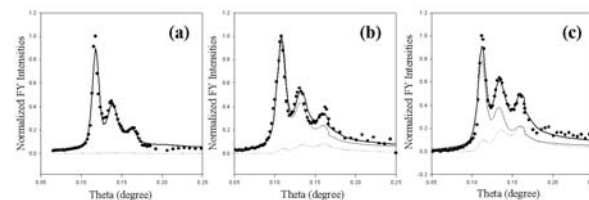


Figure 2. XSW-FY profiles of PAA/ α -Al₂O₃(1-102) samples with different Pb(II) ion concentrations ([Pb(II)] = (a) 5 x 10⁻⁸ M, (b) 5 x 10⁻⁷ M, and (c) 5 x 10⁻⁵ M) taken at an x-ray excitation energy of 14 keV.

There are fundamental differences in the chemical characteristics of organic or biofilm coatings that can occur on mineral surfaces. Biofilms are typically composed of complex mixtures of organic compounds, such as proteins, polysaccharides, fatty acids, etc., in which a variety of functional groups (e.g., carboxyl, phosphoryl, hydroxyl, and amine) are present^{26,27}. Among these the major functional groups involved in interactions with metal ions and mineral surfaces are carboxyl and phosphoryl groups²⁶ and their binding site concentrations range from 3.2 x 10⁻⁵ to 1.2 x 10⁻³ mol/g dry weight and 8.9 x 10⁻⁶ to 8.3 x 10⁻⁴ mol/g dry weight²⁸⁻³², respectively. The binding site concentrations of typical bacterial cells are much lower than those values of typical NOM (i.e. HA and FA) and PAA. Moreover, considering the typical water content (~70 wt.%) of a wet biofilm, the actual binding site concentration of the *B. cepacia* biofilm used in the previous biofilm work¹⁴ should be 2 or 3 orders of magnitudes lower than that of the PAA film used in this study. Additionally, from previous potentiometric and spectroscopic studies on the Pb(II)-PAA system, binding to ML₂-type sites has been suggested as the dominant complexation mode of PAA with divalent and trivalent cations (e.g., Pb(II)²²⁻²⁴ and Eu(III)³³); such complexes probably involve direct coordination of two carboxyl moieties to metal cation with chelation. Such sites have higher binding affinity for Pb(II) ions (log β_{102} = 6.75 - 7.00)^{22,23} compared to ML-type binding sites, which are predicted to be the dominant binding sites Pb(II) in bacterial cell walls (log K = 3.9 - 4.7).²⁸⁻

^{30,32} They also are likely to have higher affinities for Pb(II) than inner-sphere binding sites at the α -Al₂O₃(1-102) surface at pH 6 (log K_{app} = 6.0 at pH = 6)¹⁴. Therefore, aqueous Pb(II) ions should preferentially bind to carboxyl functional groups in PAA until these ML₂-type binding sites become saturated. At that point, excess Pb(II) ions should adsorb to less reactive binding sites on the α -Al₂O₃(1-102) surface. This reasoning suggests that the properties of organic coatings on mineral surfaces, including the types of binding sites, their binding affinities and site concentrations, play important roles in determining the distribution of metal (and metalloid) ions and their speciation at the mineral/organic film/water interfaces. Moreover, this comparison of biofilm and PAA coatings with different types of binding sites for Pb(II) also provides some insight about metal ion partitioning behavior in natural organic matter (i.e. humic and fulvic acids). Such acids are known to have both type of binding sites^{33,34}.

Effect of Substrate Reactivities on Lead Partitioning. The relative reactivities of organic coating-free α -Al₂O₃ (0001), α -Al₂O₃ (1-102), and α -Fe₂O₃ (0001) surfaces with respect to aqueous Pb(II) ions were previously studied using x-ray photoelectron spectroscopy and grazing-incidence XAFS methods and were shown to have the following order of reactivity: α -Fe₂O₃ (0001) > α -Al₂O₃ (1-102) > α -Al₂O₃ (0001)^{35,36}. In addition, Templeton *et al.*¹⁴ showed that the order of reactivity of these substrates with respect to aqueous Pb(II) ions is not altered by a continuous *B. cepacia* biofilm coating. However, the stability constant for the PAA-Pb(II) complex (i.e. ML₂ species) is typically larger than those of higher affinity mineral surface binding sites (i.e. M₁). Moreover, the stability constant for the higher affinity Pb(II)-humate complex (i.e. log K_{Pb-S2}) is 2.1 to 3.4 units larger than those of higher affinity mineral surface binding sites. Therefore, in the case of a mineral substrate coated by PAA or HA, it is more probable that mineral surface binding site will be “blocked” or “altered” by organic coatings with higher affinity binding sites. To test this possibility, we performed XSW-FY experiments on Pb(II) partitioning between a continuous PAA coating and α -Fe₂O₃ (0001), α -Al₂O₃ (1-102), and α -Al₂O₃ (0001) surfaces. As shown in Fig. 3, the majority of Pb(II) ions are partitioned into the PAA coating for all three metal oxide substrates, which can be explained by the higher binding affinity of ML₂ binding sites within the PAA coating. However, we also observe an increase of adsorbed Pb(II) species as the intrinsic reactivities of the metal oxide surfaces increase, indicating that the surface binding sites have not been “blocked” and the relative differences in surface reactivities with respect to Pb(II) have not been seriously altered by the presence of the PAA coating. This observation is consistent with the relative reactivities of biofilm-mineral interfaces with respect to aqueous Pb(II)¹⁴ and is also similar to the results by Zachara *et al.*³⁷ for a Co(II)-mineral-humic acid system.

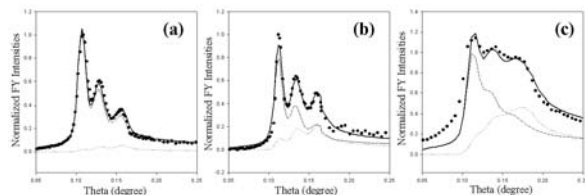


Figure 3. XSW-FY profiles of PAA/ α -Al₂O₃ (1-102) samples with different Pb(II) ion concentrations ([Pb(II)] = (a) 5×10^{-8} M, (b) 5×10^{-7} M, and (c) 5×10^{-5} M) taken at an x-ray excitation energy of 14 keV.

Acknowledgments. We wish to acknowledge the support of NSF Grants CHE-0089215 (Stanford University CRAEMS on Chemical and Microbial Interactions at Environmental Interfaces) and CHE-0431425 (Stanford Environmental Molecular Science Institute). We also wish to thank to Dr. Alexis S. Templeton, Joe Rogers, and other APS and SSRL staff members for the help with XSW-FY/x-ray reflectivity measurements. This work was performed at GSECARS (sector 13), Advanced Photon Source (APS), Argonne National Laboratory. GeoSoilEnviroCARS is supported by the National Science Foundation - Earth Sciences (EAR-0217473), Department of Energy - Geosciences (DE-FG02-94ER14466) and the State of Illinois. Use of the APS was supported by the U.S. Department of Energy, Basic Energy Sciences under Contract No. W-31-109-Eng-38.

References

- (1) Brown, G. E., Jr.; Henrich, V. E.; Casey, W. H.; Clark, D. L.; Eggleston, C.; Felmy, A.; Goodman, D. W.; Gratzel, M.; Maciel, G.; McCarthy, M. I.; Nealon, K. H.; Sverjensky, D. A.; Toney, M. F.; Zachara, J. M. *Chem. Rev.* **1999**, *99*, 77-174.
- (2) Brown, G. E., Jr.; Parks, G. A. *Internat. Geol. Rev.* **2001**, *43*, 963-1073.
- (3) Niehoff, R. A.; Loeb, G. I. *J. Marine Res.* **1974**, *32*, 5-12.
- (4) Hunter, K. A.; Liss, P. S. *Nature* **1979**, *282*, 823-825.
- (5) Baliestrieri, L.; Brewer, P. G.; Murray, J. W. *Deep Sea Res.* **1981**, *28A*, 101-121.
- (6) Davis, J. A. *Geochim. Cosmochim. Acta* **1982**, *46*, 2381-2393.
- (7) Tipping, E.; Cooke, D. *Geochim. Cosmochim. Acta* **1982**, *49*, 75-80.
- (8) Murphy, E. M.; Zachara, J. M. *Geoderma* **1995**, *67*, 103-124.
- (9) Kaiser, K.; Guggenberger, G. *Org. Geochem.* **2000**, *31*, 711-725.
- (10) Kaiser, K.; Guggenberger, G. *Europ. J. Soil Sci.* **2003**, *54*, 219-236.
- (11) Ransom, B.; Bennett, R.; Baerwald, R.; Hulbert, V.; Burkett, P. *Am. Mineral.* **1999**, *84*, 183-192.
- (12) Ransom, B.; Bennett, R.; Baerwald, R.; Shea, K. *Marine Geol.* **1997**, *138*, 1-9.
- (13) Templeton, A.; Trainor, T.; Spormann, A.; Brown, G. E., Jr. *Geochim. Cosmochim. Acta* **2003**, *67*, 3547-3557.
- (14) Templeton, A. S.; Trainor, T. P.; Traina, S. J.; Spormann, A. M.; Brown, G. E., Jr. *Proc. Nat. Acad. Sci. U. S. A.* **2001**, *98*, 11897-11902.
- (15) Wang, J.; Caffrey, M.; Bedzyk, M.; Penner, T. *J. Phys. Chem.* **1994**, *98*, 10957-10968.
- (16) Wang, J.; Bedzyk, M.; Caffrey, M. *Science* **1992**, *258*, 775-778.
- (17) Wang, J.; Caffrey, M. *J. Amer. Chem. Soc.* **1995**, *117*, 3304-3305.
- (18) Trainor, T. P.; Templeton, A. S.; Brown, G. E., Jr.; Parks, G. A. *Langmuir* **2002**, *18*, 5782-5791.
- (19) Libera, J. A.; Gurney, R. W.; Nguyen, S. T.; Hupp, J. T.; Liu, C.; Conley, R.; Bedzyk, M. J. *Langmuir* **2004**, *20*, 8022-8029.
- (20) Yoon, T. H.; Trainor, T. P.; Eng, P. J.; Bargar, J. R.; Brown, G. E. Jr., *Langmuir* (in revision), **2005**.
- (21) Franks, G.; Meagher, L. *Colloids Surf. A* **2003**, *214*, 99-110.
- (22) Hayashi, H.; Komatsu, T. *Bull. Chem. Soc. Japan* **1991**, *64*, 303-305.
- (23) Morlay, C.; Cromer, M.; Mougnot, Y.; Vittori, O. *Talanta* **1999**, *48*, 1159-1166.
- (24) Miyajima, T.; Mori, M.; Ishiguro, S. *J. Colloid Interface Sc.* **1997**, *187*, 259-266.
- (25) Arai, Y.; Elzinga, E. J.; Sparks, D. L. *J. Colloid Interface Sc.* **2001**, *235*, 80-88.
- (26) Flemming, H. C. *Water Sci Technol.* **1995**, *32*, 27-33.
- (27) Watnick, P.; Kolter, R. *J. Bacteriol.* **2000**, *182*, 2675-2679.
- (28) Yee, N.; Benning, L.; Phoenix, V.; Ferris, F. G. *Environ. Sci. Technol.* **2004**, *38*, 775-782.
- (29) Ngwenya, B.; Sutherland, I.; Kennedy, L. *Appl. Geochem.* **2003**, *18*, 527-538.
- (30) Fein, J.; Daughney, C.; Yee, N.; Davis, T. *Geochim. Cosmochim. Acta* **1997**, *61*, 3319-3328.
- (31) Haas, J.; Dichristina, T.; Wade, R. *Chem. Geol.* **2001**, *180*, 33-54.
- (32) Daughney, C.; Fein, J.; Yee, N. *Chem. Geol.* **1998**, *144*, 161-176.
- (33) Yoon, T. H.; Moon, H.; Park, Y. J.; Park, K. K. *Environ. Sci. Technol.* **1994**, *28*, 2139-2146.
- (34) Liu, A.; Gonzalez, R. *Langmuir* **2000**, *16*, 3902-3909.
- (35) Bargar, J. R.; Towle, S. N.; Brown, G. E., Jr.; Parks, G. A. *Geochim. Cosmochim. Acta* **1996**, *60*, 3541-3547.
- (36) Bargar, J. R.; Towle, S. N.; Brown, G. E., Jr.; Parks, G. A. *J. Colloid Interface Sci.* **1997**, *185*, 473-492.
- (37) Zachara, J. M.; Resch, C. T.; Smith, S. C. *Geochim. Cosmochim. Acta* **1994**, *58*, 553-566.